

Landslide Susceptibility Modelling of Central Highland Part of Chaliyar River Basin, Kerala, India with Integrated Algorithms of Frequency Ratio and Shannon Entropy

Suraj P.R.*¹, Melvin Babu, Manoharan A.N., Archana Krishnan N., Shruthi Mayya K. and Niveditha P.

Department of Geology, Government College, Kasaragod-671123 (KL), India

(*Corresponding Author, E-mail: sprbhoomi@gmail.com)

Abstract

An integrated landslide susceptibility analysis is carried out for the central highland region of the Chaliyar River Basin in Kerala, India using bivariate statistical methods, namely the Frequency Ratio (FR) and Shannon Entropy (SE). The study addresses the complex nature of landslides, influenced by natural as well as anthropogenic factors, with specific focus on assessing the landslide likelihood of the study area. The methodology involves a systematic approach of collecting the inventory data, identifying various landslide causative factors and developing their corresponding thematic maps, spatial analysis of landslide occurrence and causative factors using GIS software and generation of Landslide Susceptibility Model (LSM) employing FR and SE algorithm, followed by model validation. Various causative factors considered for the study include slope angle, slope aspect, slope curvature, elevation, lithology, drainage density, land use and land cover (LULC), Topographic Wetness Index (TWI) and Normalized Difference Vegetation Index (NDVI). The FR and SE algorithm enable the spatial classification of the study area into four landslide susceptibility categories namely Low, Moderate, High, and Very High. Validation of both the LSMs was carried out using Landslide Density Index (LDI) and Area Under the Curve (AUC) methods. LDI demonstrate a positive fit for both the models, which is indicative of reliability of the susceptibility predictions of the study area. A slightly higher AUC value of SE model is an indication of a high accuracy rate of SE model over FR model. This research brings out a robust methodology for predicting and identifying the landslide risks of the study area. The outcomes of this study will help in developing effective strategies to manage the landslide hazards in geologically vulnerable areas.

Keywords: Landslide Susceptibility, Landslide Conditioning Factors, Frequency Ratio, Shannon Entropy, Landslide Density Index (LDI), Area Under the Curve (AUC)

Introduction

Landslides, recognized as profoundly calamitous natural events, unleash deleterious consequences on both the physical and human spheres (Bui *et al.*, 2020). Beyond the immediate physical devastation, these occurrences cast an enduring economic and social impact over human habitats (Hong *et al.*, 2017). Global statistics from 1995 to 2014 depict a staggering toll of 3,876 reported landslides, resulting in 11,689 injuries and 163,658 fatalities (Haque *et al.*, 2019). India is highly vulnerable to landslide and related disasters. Recent studies show that Northwest Himalayas contribute 66.5% of landslides, followed by the Northeast Himalayas (18.8%) and the Western Ghats (14.7%) in India (Martha *et al.*, 2021). The peculiar geographical location of Kerala makes the state a highly vulnerable to landslide and related natural disasters. In 2018 monsoon season alone, 4,728 cases of landslide occurrences were reported from the state (Hao *et al.*, 2020). These figures underscore the imperative to identify high-risk

landslide zones and implement proactive measures for prevention and mitigation to safeguard communities globally as well as locally.

Recently, researchers are widely using the Machine Learning algorithm in landslide susceptibility modelling such as support vector machine, multivariate adaptive regression spline, boosted regression, classification and regression trees, quadratic discriminant analysis, artificial neural networks, maximum entropy, random forest, and generalized linear model (Ali *et al.*, 2022). At the same time, various bivariate and multivariate statistical methods are still widely employed in Landslide Susceptibility analysis and hazard zonation (Mengistu *et al.*, 2019; Hamza and Raghuvanshi, 2017; Girma *et al.*, 2015) because of its simplicity. The bivariate approach, grounded in inductive logic, state that if a situation holds in all observed cases, it holds universally (Dai and Lee, 2001). Frequency Ratio (FR) analysis, a common method among bivariate statistical approaches, correlates responsible causative factor classes with the spatial distribution of past landslides (Chimidi *et al.*, 2017; Hamza and Raghuvanshi, 2017; Girma *et al.*, 2015; Lee and Min, 2001). Shannon Entropy (SE) method, another bivariate statistical approach, assesses the extent to which various factors influence landslide development,

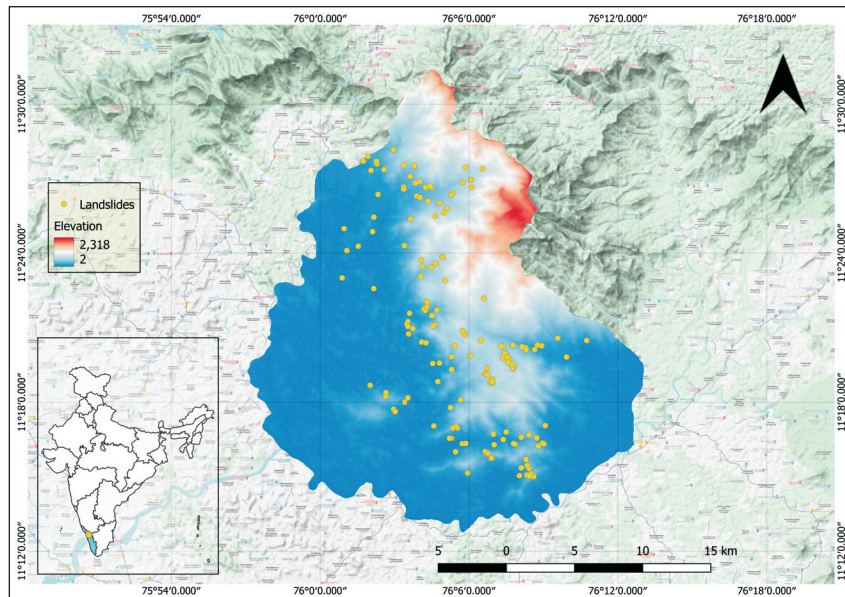


Fig.1. Location map of the study area

determining objective weights for the index system (Yang and Qiao, 2010). In the present study, efforts were made to apply Frequency Ratio (FR) and Shannon Entropy (SE) statistical algorithm to identify the landslide-susceptible zones in the central highland part of the Chaliyar River Basin, Kerala. By employing these techniques, we enhance our ability to predict and identify the vulnerability of landslides and related disasters.

Study Area

The study area encompasses the central highland portion of the Chaliyar River basin, covering an area of 583.976 km² and geographically located between latitudes 11°06'07" N and 11°33'35" N and longitudes 75°48'45" E and 76°33'00" E (Fig.1). The area is specifically constituting the key sub-watersheds of Chaliyar River namely Iruvizhinji and Kuruman. Both these tributary systems flow through Kozhikode and Malappuram districts and converge to main Chaliyar River before culminating its discharge into the Lakshadweep Sea (Ambili and Narayana, 2010). Physiographically, the study area forms the highland and midland part of Kerala, with its eastern boundary associated with the Western Ghats. The average elevation of the study area is approximately 200 meters and characterized by rugged topography in the eastern part. Geologically, majority of the area is acid to intermediate charnockite with hornblende biotite gneiss. While natural forests dominate the eastern side, agricultural and urban anthropogenic settings are more prominent land use pattern in the western side. Generally, a tropical humid climate is experienced in the study area with northeast and southwest monsoons evenly distributed. This Chaliyar Basin has garnered attention due to a high incidence of landslides in recent years, especially during the monsoon season (Fig.1). The seasonal occurrences of landslide associated with monsoon season, underscore rainfall as an external trigger contributing to these occurrences. This study aims to comprehensively analyse the landslide occurrences and various causative factors and help to identify the vulnerable area which can contribute to enhance landslide disaster management strategies locally.

Materials and Methods

The methodological flowchart of the present study is given in the Fig.2.

Landslide Inventory

A landslide inventory is a repository of historical data, capturing their geographical locations and extents. This dataset is plays a pivotal role in generating vulnerability models and later validating the model. In the present study, landslide inventory data were prepared, leveraging a multifaceted approach combining data retrieved from various online sources and field visits. This comprehensive effort resulted in identifying 176 landslides, each pinpointed and represented as a point feature on the inventory map. This dataset was then partitioned into two segments: training and a testing dataset. The 70% of the training dataset was used in constructing the Landslide Susceptibility Model (LSM), using in the ArcGIS 10.5 software and the remaining 30% of the database was used for validating the LSM efficacy.

Frequency Ratio (FR)

The Frequency Ratio (FR) is a robust and straightforward

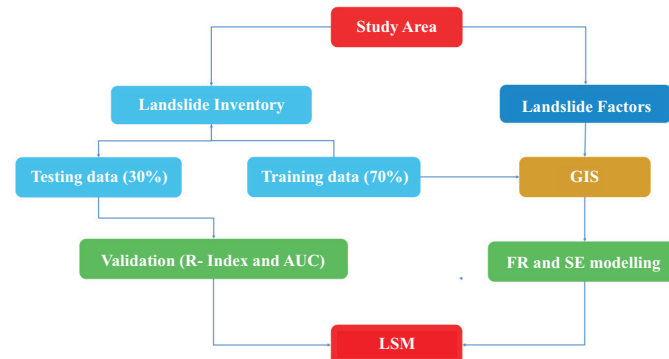


Fig.2. Methodological flow chart

bivariate statistical algorithm widely employed in landslide susceptibility mapping. This method establishes a correlation between the occurrence of landslides and the influencing factors within a study area (Girma *et al.*, 2015). The FR model quantifies the spatial relationship between past landslide locations and the various classes within a thematic layer. It is calculated as the ratio of the area or location where landslides occurred to the total study area. A value greater than 1 indicates a higher correlation, while a value less than 1 indicates a lower correlation. In order to derive the Landslide Susceptibility Index (LSI), the frequency ratio values of each thematic layer are summed (Lee and Talib, 2005; Lee and Pradhan, 2007).

Mathematically, the Frequency Ratio (FR) is calculated as follows:

$$\text{Frequency Ratio} = \text{Slide ratio} / \text{Class ratio} \quad (1)$$

Where Slide ratio =

$$\frac{\text{Number of landslide grids in a class}}{\text{Total number of landslide grids}} \times 100 \quad (2)$$

Class ratio =

$$\frac{\text{Number of grids in an individual class}}{\text{Total number of grids in the entire class}} \times 100 \quad (3)$$

$$\text{LSI} = \sum \text{FR} \quad (4)$$

Shannon Entropy (SE)

In landslide and other hazard studies, the Shannon Entropy (SE) model is utilised for weighted index calculation (Nohani *et al.*, 2019). An advancement over the Frequency Ratio model, the SE model considers the weightage of sub-factors and quantifies the instability or uncertainty within the system (Shrivastava and Panchal, 2022). SE assesses the potential impact of each contributing factor on landslide occurrence. Higher SE values indicate a more significant impact of factors on landslide occurrence.

The following equations characterise the SE model:

$$P_{ij} = \text{FR} / \sum_{i=1}^m \text{FR} \quad (1)$$

$$\sum_{i=1}^m E_{ij} = \sum_{i=1}^m (P_{ij}) \times (\ln P_{ij}) \quad (2)$$

$$H_{ij} = I + \sum_{i=1}^m E_{ij} \quad (3)$$

$$W_j = H_{ij} / \sum_{i=1}^n H_{ij} \quad (4)$$

P_{ij} is the probability density, and FR is the frequency ratio of sub-factors. W_j is the weightage of causative factors obtained from Shannon's entropy technique. These values can then assign weight to causative factors, while frequency ratio values are used for sub-factors.

Validation methods

Two types of validation and accuracy evaluation of bivariate statistical models were carried out using 30% testing data which was randomly selected from the landslide inventory during the spatial modelling process.

Relative Landslide Density Index or R -Index

The accuracy of the output of the LSM model generated by the FR and SE method is validated through Relative

Landslide Density Index or R – Index. It assesses the relationship between the landslide validation database and the LSM result (Meena *et al.*, 2019). The following equation calculates the R-index-

$$R = (n_i/N_i) / \sum (n_i/N_i) \times 100 \quad (9)$$

Where,

n_i is the percentage of the landslide in each susceptible class

N_i is the percentage of the landslide-susceptible area in each landslide-susceptible class.

This metric provides insights into the alignment between predicted susceptibility and actual landslide locations.

Area Under the Curve (AUC)

The Area Under the Curve (AUC) of the Receiver Operating Characteristic (ROC) is a widely recognised and highly regarded validation measure, is commonly employed in natural hazard assessment (Begueria, 2006). It is one of the most frequently used qualitative accuracy assessment methods for predictive models in natural hazard assessment (Pradhan and Lee, 2009). An ideal model shows an AUC value close to 1.0, whereas a value close to 0.5 indicates inaccuracy in the model (Fawcett, 2006).

Factors Affecting Landslide

Understanding the factors influencing landslides is crucial for effective risk assessment and mitigation. While there is ongoing debate on the optimal selection of these factors for landslide studies (Hong *et al.*, 2017), our research focuses on nine key variables: slope angle, slope aspect, slope curvature, elevation, drainage density, geology, Land Use Land Cover, Total Wetness Index (TWI) and Normalised Vegetation Index (NDVI). These factors were chosen based on the local geo-environmental setup to ensure a comprehensive analysis. The data sources for different landslide conditioning factors are given in Table 1.

Slope

Landslides bear a direct correlation with slope angle, a pivotal parameter widely employed in the formulation of landslide susceptibility maps (Lee and Min, 2001; Saha *et al.*, 2005; Yalcin, 2011). This parameter exerts a predominant influence over both the spatial distribution and the magnitude of landslide occurrences. The slope angle of the study area is categorized into five distinct classes: 0° to 15° , 15° to 29° , 29° to 44° , 44° to 58° and 58° to 72° (Fig.3a). This classification was achieved through the application of the natural breaks classification method within the Geographic Information System (GIS).

Table 1: Data source for different landslide conditioning factors

No	Data	Source
1	Slope	ASTER DEM
2	Aspect	ASTER DEM
3	Curvature	ASTER DEM
4	Elevation	ASTER DEM
5	Drainage Density	ASTER DEM
6	Lithology	Bhukosh data/ https://www.gsi.gov.in/webcenter/portal
7	LULC	LANDSAT - 8
8	TWI	ASTER DEM
9	NDVI	Sentinel 2A

Table 2: FR and SE values of landslide conditioning factors of the study area

Factors	Class	No. of Landslide	% of Landslide	Area no	% Area	FR	FRn	Sum of FR	Sum of %FR	Pij	Eij	Hij	Wj
SLOPE (degree)	0 - 8.7	9	7.317	203398	31.347	0.233	0.129	5.081	12.390	0.046	-0.061	0.369	0.097
	8.7 - 17	43	34.959	185857	28.643	1.221	0.675			0.240	-0.149		
	17 - 26	47	38.211	137212	21.146	1.807	1.000			0.356	-0.160		
	26 - 37	20	16.260	89442	13.784	1.180	0.653			0.232	-0.147		
	37 - 72	4	3.252	32955	5.079	0.640	0.354			0.126	-0.113		
		123		648864		5.081				1.000	-0.631		
ASPECT	Flat (-1)	0	0.000	339	0.052	0.000	0.000	7.901	19.268	0.000	0.000	0.103	0.027
	North (0.00-22.54)	13	10.569	67177	10.353	1.021	0.846			0.129	-0.115		
	Northeast (22.5-67.5)	11	8.943	64700	9.971	0.897	0.743			0.114	-0.107		
	East (67.5-112.5)	10	8.130	63954	9.856	0.825	0.684			0.104	-0.102		
	Southeast (112.5-157.5)	11	8.943	76100	11.728	0.763	0.632			0.097	-0.098		
	South (157.5-202.5)	17	13.821	102229	15.755	0.877	0.727			0.111	-0.106		
	Southwest (202.5-247.5)	25	20.325	110024	16.956	1.199	0.993			0.152	-0.124		
	West (247.5-292.5)	19	15.447	90025	13.874	1.113	0.923			0.141	-0.120		
	Northwest (292.5-337.5)	17	13.821	74316	11.453	1.207	1.000			0.153	-0.125		
		123		648864		7.901				1.000	-0.897		
CURVATURE	Concave (-31.77 - -0.005)	68	55.28	314947	48.54	1.14	1.000	2.559	6.24	0.445	-0.156	0.544	0.143
	Flat (-0.005 - 0.005)	3	2.44	30731	4.74	0.51	0.452			0.201	-0.140		
	Convex (0.005 - 31)	52	42.28	303186	46.73	0.90	0.794			0.354	-0.160		
		123		648864		2.559				1.000	-0.456		
ELEVATION (m)	2 - 203	49	39.837	367254	56.600	0.704	0.353	4.669	11.385	0.151	-0.124	0.560	0.147
	203 - 524	38	30.894	101846	15.696	1.968	0.986			0.422	-0.158		
	524 - 926	36	29.268	95117	14.659	1.997	1.000			0.428	-0.158		
	926 - 1,450	0	0.000	56736	8.744	0.000	0.000			0.000	0.000		
	1,450 - 2,320	0	0.000	27911	4.302	0.000	0.000			0.000	0.000		
		123		648864		4.669				1.000	-0.440		
DRAINAGE DENSITY	0.441 - 2.98	1	0.813	40999	6.319	0.129	0.107	4.433	10.809	0.029	-0.045	0.360	0.094
	2.98 - 4.02	26	21.138	140397	21.637	0.977	0.809			0.220	-0.145		
	4.02 - 4.72	44	35.772	214207	33.013	1.084	0.897			0.244	-0.150		
	4.72 - 5.48	36	29.268	183375	28.261	1.036	0.857			0.234	-0.148		
	5.48 - 7.61	16	13.008	69886	10.771	1.208	1.000			0.272	-0.154		
		123		648864		4.433				1.000	-0.640		
LITHOLOGY	Acid to Intermediate Charnockite	88	71.545	426461	65.724	1.089	0.362	4.916	11.989	0.221	-0.145	0.595	0.156
	Hornblende-Biotite Gneiss	34	27.642	219636	33.849	0.817	0.271			0.166	-0.129		
	Laterite	0	0.000	729	0.112	0.000	0.000			0.000	0.000		
	Sillimanite-Kyanite-Quartz Schist	1	0.813	1752	0.270	3.011	1.000			0.612	-0.130		
	Pebble Red	0	0.000	165	0.025	0.000	0.000			0.000	0.000		
	Banded Iron Formation	0	0.000	100	0.015	0.000	0.000			0.000	0.000		
	Gabbro	0	0.000	21	0.003	0.000	0.000			0.000	0.000		
		123		648864		4.916				1.000	-0.405		
LULC	Forest	91	73.984	450502	69.429	1.066	1.000	3.410	8.315	0.313	-0.158	0.536	0.141
	Agriculture	14	11.382	83329	12.842	0.886	0.832			0.260	-0.152		
	Waterbody	0	0.000	4661	0.718	0.000	0.000			0.000	0.000		
	Urban	2	1.626	20231	3.118	0.522	0.489			0.153	0.000		
	Barren_Land	16	13.008	90141	13.892	0.936	0.879			0.275	-0.154		
		123		648864		3.410				1.000	-0.464		
TWI	2.24 - 5.57	52	42.276	257515	39.687	1.065	0.768	4.316	10.526	0.247	-0.150	0.340	0.089
	5.57 - 7.56	43	34.959	241843	37.272	0.938	0.676			0.217	-0.144		
	7.56 - 10.5	22	17.886	83691	12.898	1.387	1.000			0.321	-0.158		
	10.5 - 14.4	5	4.065	53696	8.275	0.491	0.354			0.114	-0.107		
	14.4 - 22.4	1	0.813	12119	1.868	0.435	0.314			0.101	-0.100		
		123		648864		4.316				1.000	-0.660		
NDVI	-0.14 - 0.23	6	4.878	46415	7.153	0.682	0.628	3.722	9.077	0.183	-0.135	0.404	0.106
	0.23 - 0.35	30	24.390	170329	26.250	0.929	0.856			0.250	-0.150		
	0.35 - 0.45	54	43.902	262349	40.432	1.086	1.000			0.292	-0.156		
	0.45 - 0.64	33	26.829	169771	26.164	1.025	0.944			0.275	-0.154		
		123		648864		3.722				1.000	-0.596		

Slope Aspect

Slope aspect plays role in the landslide vulnerability highlighted by Hong *et al.* (2017a) as it is function of the amount sun light, influence of wind, and precipitation received by the area (Yu and Gao, 2020). In our study, the orientation of slopes within the study area is categorised into nine directional classes (Fig. 3b). These classes consist of North (337.5° - 22.5°), NE (22.5° - 67.5°), E (67.5° - 112.5°), SE (112.5° - 157.5°), S (157.5° - 202.5°), SW (202.5° - 247.5°), W (247.5° - 292.5°), NW (292.5° - 337.5°) and a Flat (-1).

Slope Curvature

The Earth's surface curvature is illustrated in our study through plane and profile curvature, as both factors are crucial in influencing surface and groundwater infiltration. This, in turn, significantly impacts surface and subsurface erosion (Hong *et al.*, 2017a). Utilizing DEM, curvature map for the study area was created, classifying slopes into concave, convex, and flat categories (Fig. 3c).

Elevation

The elevation of an area stands out as a significant factor influencing landslide susceptibility (Hong *et al.*, 2017b). In essence, higher elevations tend to exhibit increased landslide likelihood, influenced by factors such as rainfall volume, slope characteristics, and the type and density of vegetation. To delineate these elevation-related patterns, our study divides the study area into five distinct elevation classes. This classification is derived from DEM data using natural breaks in GIS (Fig. 3d).

Lithology

The lithological map of the study area was compiled from a 1:50,000 scale geological map published by the Geological Survey of India (2013). Notably, the study area's major lithological units are acid to intermediate Charnokite and Hornblende Biotite Gneiss (Fig. 3e).

Drainage Density

The occurrence of landslides is significantly shaped by the drainage features of a region (Bahrami *et al.*, 2020). This influence becomes evident in scenarios where the erosion caused by river water at the base of the slope compromises its stability (Uchenna *et al.*, 2023). In this study, we classified drainage density into five specific levels, ranging from low to high (Fig. 3f).

Land Use and Land Cover (LULC)

Changing land use and land cover play a significant role in landslide occurrence of a terrain (Renata *et al.*, 2023). Normally, good vegetative cover is relatively stable whereas improper land use may cause the slope instability thereby landslide (Panchal and Shrivastava, 2022). LULC map of the study area was extracted from LANDSAT – 8 Imagery, using the supervised learning technique in Arc GIS 10.5. The observation reveals that the study area is predominantly covered by forests, agricultural land, barren land and water bodies (Fig. 3g).

Topographic Wetness Index (TWI)

The Topographic Wetness Index (TWI) is a modelling

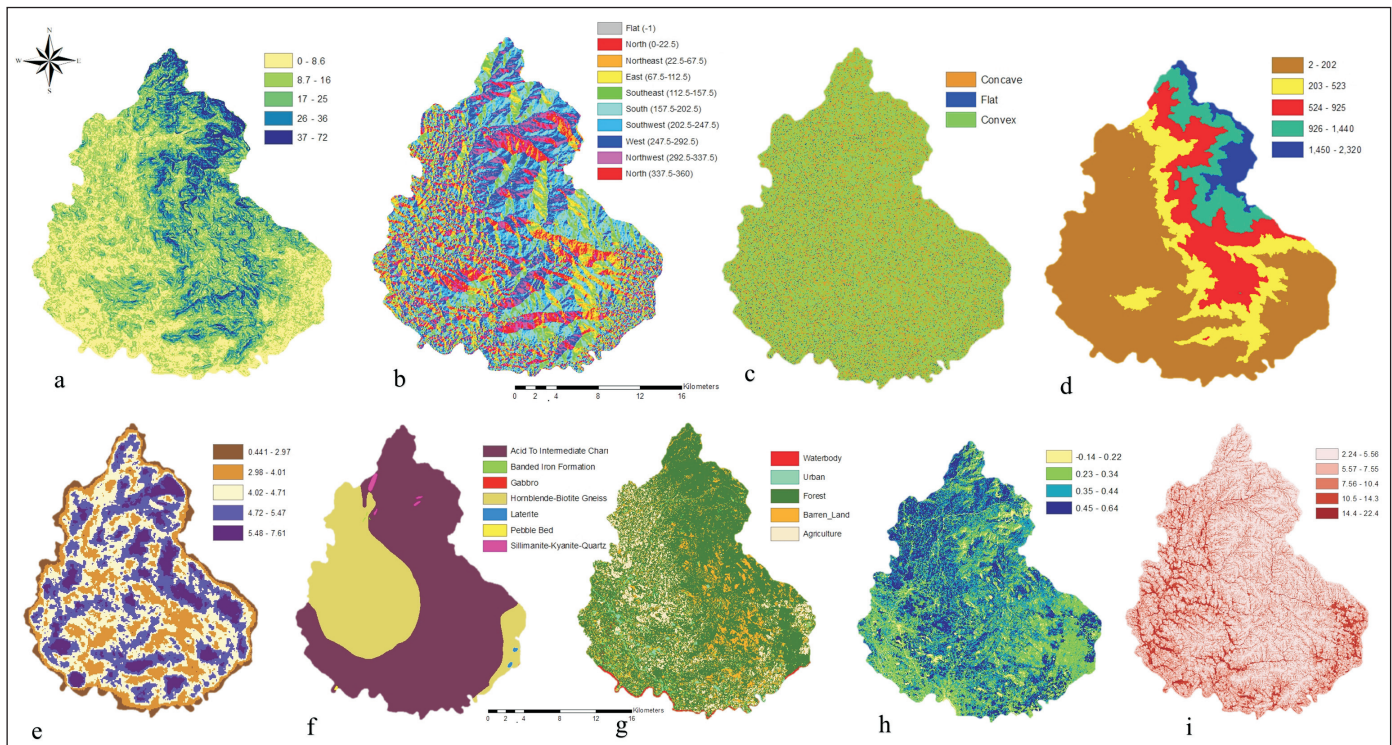


Fig.3. Thematic map landslide conditioning factors: (a) Slope (b) Slope Aspect (c) Slope Curvature (d) Elevation (e) Lithology (f) Drainage Density (g) Land Use Land Cover (h) Normalised Vegetation Index (i) Topographic Wetness Index

parameter used to estimate a landscape's potential wetness or soil moisture content based on its topography. It plays a significant role in the LSM analysis. It is computed using the following formula;

$$\text{TWI} = \ln \cotan\beta$$

Where, α - catchment area ; $\tan\beta$ - slope gradient

The TWI for the study area is divided into five classes (Fig. 3h). The maximum TWI value is 22.4, and the minimum value is 2.24.

Normalised Difference Vegetation Index (NDVI)

The Normalised Difference Vegetation Index (NDVI) is a standardised index used to quantify an area's greenness (relative biomass). It relies on the differential reflection of light in the red and near-infrared bands to monitor the density and vigour of green vegetation growth through the spectral response to solar radiation. It is calculated using the following equation.

$$\text{NDVI} = [(IR-R)/(IR+R)]$$

Where IR = Pixel value from infrared band

R = Pixel value from red band

Negative values typically indicate clouds and water, positive values near zero signify bare soil, and higher positive values reflect varying degrees of vegetation density. In the study area, NDVI values ranges from -0.14 to 0.64 (Fig. 3i).

Results and Discussion

Table 2 shows the result of the landslide susceptibility analysis of the landslide affecting parameters using FR and SE algorithm. The result shows that highest number of landslide occurrences is observed in three slope classes i.e., between 8 to 37 degrees with FR value of 1.221, 1.807 and 1.180 and Pij value of 0.240, 0.356 and 0.232. The low occurrence of landslides in higher slope classes of the study area is due to absence of thick soil cover and bed rock exposure.

The maximum landslide density is found in the north west aspect of the study area with the highest FR value of 1.207 and Pij value of 0.153. Next to that, the maximum landslide is documented (Table 1) in the southwest, west and north aspect, which is attributed to high humidity climatic condition and a relatively higher moisture content of the soil.

The results of slope curvature (topographic morphology) show that the maximum landslide density is associated with concave and convex slopes compared to flat regions. The maximum observed FR value is 1.14 for concave slope and 0.90 for convex slope, whereas the observed Pij value is 0.445 for concave slope and 0.354 for convex slope. Negative topographic curvature can hold more water than positively curved terrain, resulting in relative increase in soil wetness.

The probability of landslide occurrence for various classes of drainage density was also calculated using FR and SE algorithm. It is observed that maximum landslide occurrence is associated with higher drainage density in the study area. The higher drainage density class such as 4.02 – 4.72, 4.72 – 5.48 and 5.48 – 7.61 has the maximum FR value of 1.08, 1.036 and 1.208 and Pij value of 0.244, 0.234 and 0.272, respectively.

In general, higher the elevation coupled with high angle slope of the terrain, the probability of landslide occurrence is higher. The maximum landslide occurrence in the study area is observed

between 203 – 523 m and 524 – 925 m elevation classes with FR value of 1.986 and 1.997 and Pij value of 0.422 and 0.428, respectively. This is mainly due to the presence of thick soil cover with high angle slope in the moderately elevated terrain. The conspicuous absence of landslide occurrence in highly elevated part of the study area is due to the absence of thick soil cover with low to moderate slope angle.

Acid to intermediate charnokoite, hornblede biotite gneiss and sillimanite bearing schistose rocks are the major rock types of the study area. From FR and SE analysis it is found that maximum landslide occurrence is reported from Sillimanite Schist with FR value of 3.011 and Pij value of 0.612 followed by Charnokite with FR value of 1.089 and Pij value of 0.221.

Land Use and Land Cover (LULC) and its influence on the past landslide occurrence were also analysed here. It is observed that maximum landslides occurred in the forest area indicated by the FR value of 1.066 and Pij value of 0.313. Next to that the most landslide occurrence is associated with barren and agricultural lands with FR values of 0.879 and 0.886 and Pij value of 0.275 and 0.260, respectively.

The Topographic Wetness Index (TWI) of the study area ranges from 2.24 to 22.4. The wetness class of 7.56 – 10.4 shows the maximum landslide susceptibility as indicated by the FR (1.387) and Pij (0.321) values.

The study area is divided into various NDVI classes and the probability of each class and their relation to landslide occurrence is given in the Table 2. The maximum FR and Pij value of 1.068 and 0.292 are observed for the NDVI class of 0.35 to 0.44 and next higher FR and Pij value 1.025 to 0.275 is observed for NDVI class of 0.45 to 0.6. Higher NDVI values with higher FR and Pij values indicate that landslide occurrences are more associated with forested land.

Development of Landslide Susceptibility Map

The FR and SE algorithms were used to determine the weight of each class for various conditioning factors. These weights were then applied in GIS to create Landslide Susceptibility Models (LSMs) for the study area (Fig. 4). These models categorize the area into Low, Moderate, High, and Very Highland slide susceptible classes using natural breaks in Arc GIS. As per the FR algorithm, 7.8% of the study area falls into the Low susceptibility class, while the SE algorithm gives a higher percentage of 20.2 for low

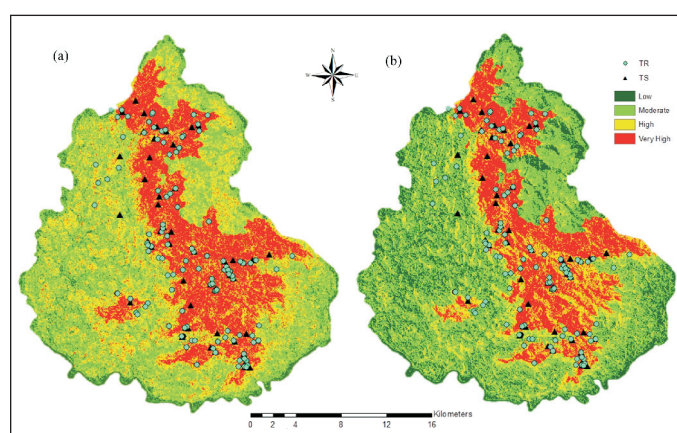


Fig.4. Landslide Susceptibility Map: (a) Frequency Ratio (b) Shannon Entropy

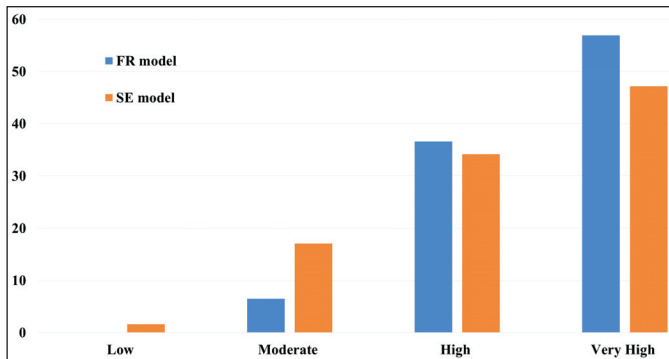


Fig.5. Distribution of landslide percentage in each susceptibility class

susceptible class. Moderate susceptibility areas account for 30.5% (FR) and 35.5% (SE). High susceptibility areas make up to 36% (FR) and 23% (SE), and Very High susceptibility areas cover 25.7% (FR) and 21.2% (SE). It is observed that 93.5% of landslides of the study area are restricted to very high and high susceptibility zones as per FR algorithm, while inference from SE algorithm indicates that 81.3% of all reported landslides are restricted to high and very high susceptible zone (Fig.5).

Validation of Landslide Susceptibility Models (LSMs)

In this study, the Relative Landslide Density Index (R-Index) and Area Under the Curve (AUC) of ROC were used to evaluate the effectiveness of the FR and SE algorithms in determining the landslide susceptibility. The R-Index curve for both models were positive, indicating the reliability of the generated landslide susceptibility predictions (Fig. 6 a). The AUC values for the FR and SE models were 0.8339 and 0.8387, respectively (Fig. 6b). Notably, the AUC value for the Landslide Susceptibility Model (LSM) produced by the SE algorithm was slightly higher than that of the FR model. This suggests that the SE algorithm demonstrates a marginally higher level of reliability in determining landslide susceptibility compared to the FR algorithm.

Conclusions

The Landslide Susceptibility Models (LSMs) were generated for central highland part of the Chaliyar River Basin of Kerala, India using FR and SE algorithms. The generated LSM classifies the study area into Low, Moderate, High, and Very High landslide susceptibility zones. The FR and SE models identified that 93.5% and 81.3% of the study area respectively are Very High and High susceptible zones. For validating both the LSMs, Relative Landslide Density Index (R-Index) and Area Under the Curve (AUC) method were used. The positive R-Index curves affirm the reliability of the generated landslide susceptibility models using both FR and SE models. Both the models have higher AUC values, but a relatively higher AUC value is observed for SE (0.8387) as compared to the value of FR model (0.8339). The results underscore the necessity of considering both algorithms for a comprehensive understanding of landslide susceptibility of a terrain. The emphasis

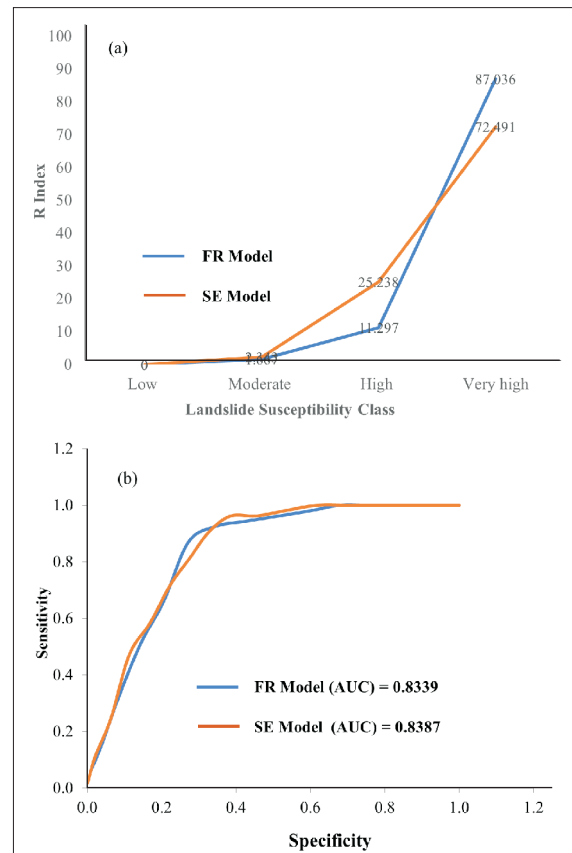


Fig.6. Validation curve using (a) Relative Landslide Density Index (b) Area Under the Curve (AUC)

on integrating multiple causative factors in GIS-based LSMs contributes valuable insights for land-use planning and disaster preparedness in the study area.

Author's Contributions

SPR: Conceptualization, Original Manuscript Drafting, Investigation, Methodology, Formal Analysis. **MB:** Investigation, Software Handling. **MAN:** Reviewing and Editing. **AKN:** Editing and Software Support. **SMK:** Editing and Software Support. **NP:** Editing and Software Support.

Conflict of Interest

The authors declare that there is no conflict of interest.

Acknowledgements

The authors would like to thank the Department of Geology, Government College, Kottayam, Kerala for supporting with GIS software. The authors would also like to thank Dr. Ananthapadmanabha A. L., Associate Professor of the Department of Geology, Government College, Kasaragod, Kerala for his valuable suggestions to improve the language of the manuscript.

References

- Ambili, V. and A.C. Narayana. (2010). Evolution of Chaliyar river drainage basin: Insights from tectonic geomorphology. PhD diss., Cochin University of Science and Technology, pp.120-124.
- Ali, S.A., Parvin, F., Vojteková, J., Costache, R., Linh, N.T.T., Pham, Q.B., Vojtek, M., Gigović, L., Ahmad, A. and Ghorbani, M.A. (2021). GIS-based landslide susceptibility modeling: A comparison between fuzzy multi-criteria and machine learning algorithms. *Geosci. Front.*, v. 12(2), pp.857-876. <https://doi.org/10.1016/j.gsf.2020.09.004>.
- Bahrami, S., Rahimzadeh, B. and Khaleghi, S. (2020). Analyzing the effects of tectonic and lithology on the occurrence of landslide along Zagros ophiolitic suture: A case study of Sarv-Abad, Kurdistan, Iran. *Bull. Engineer. Geol. Environ.*, v.79, pp.1619-1637. <https://doi.org/10.1007/s10064-019-01639-3>.
- Beguería, S. (2006). Validation and evaluation of predictive models in hazard assessment and risk management. *Nat. Hazar.*, v.37, pp.315-329. <https://doi.org/10.1007/s11069-005-5182-6>.
- Bui, D.T., Tsangaratos, P., Nguyen, V.T., Van Liem, N. and Trinh, P.T. (2020). Comparing the prediction performance of a Deep Learning Neural Network model with conventional machine learning models in landslide susceptibility assessment. *Catena*, v. 188, p. 104426. <https://doi.org/10.1016/j.catena.2019.104426>.
- Chimidi, G., Raghuvanshi, T.K. and Suryabagavan, K.V. (2017). Landslide hazard evaluation and zonation in and around Gimbi town, western Ethiopia—a GIS-based statistical approach. *Appl. Geomat.*, v. 9, pp. 219-236. <https://doi.org/10.1007/s12518-017-0195-x>.
- Dai, F.C. and Lee, C.F. (2001). Terrain-based mapping of landslide susceptibility using a geographical information system: a case study. *Canad. Geotech. Jour.*, v. 38(5), pp.911-923. <https://doi.org/10.1139/t01-021>.
- Fawcett, T. (2006). An introduction to ROC analysis. *Patter. Recog. Lett.*, v. 27(8), pp.861-874. <https://doi.org/10.1016/j.patrec.2005.10.010>
- Girma, F., Raghuvanshi, T.K., Ayenew, T. and Hailemariam, T. (2015). Landslide hazard zonation in Ada Berga District, Central Ethiopia—a GIS based statistical approach. *Jour. Geom.*, v. 9(1), pp.25-38.
- Hamza, T. and Raghuvanshi, T.K. (2017). GIS based landslide hazard evaluation and zonation—A case from Jeldu District, Central Ethiopia. *Jour. King Saud Univer.-Sci.*, v. 29(2), pp.151-165.
- Haque, U., Da Silva, P.F., Devoli, G., Pilz, J., Zhao, B., Khaloua, A., Wilopo, W., Andersen, P., Lu, P., Lee, J. and Yamamoto, T. (2019). The human cost of global warming: Deadly landslides and their triggers (1995–2014). *Sci. Tot. Environ.*, v. 682, pp.673-684. <https://doi.org/10.1016/j.scitotenv.2019.03.415>.
- Hao, L., Van Westen, C., KS, Sajinkumar, Martha, T.R., Jaiswal, P. and McAdoo, B. (2020). Constructing a complete landslide inventory dataset for the 2018 monsoon disaster in Kerala, India, for land use change analysis. *Earth Syst. Sci. Data Discuss.*, v.12, pp.1-32. <https://doi.org/10.5194/esd-12-2899-2020>.
- Hong, H., Chen, W., Xu, C., Youssef, A.M., Pradhan, B. and Tien Bui, D. (2017a). Rainfall-induced landslide susceptibility assessment at the Chongren area (China) using frequency ratio, certainty factor, and index of entropy. *Geocart. Internationl.*, v.32(2), pp.139-154. <https://doi.org/10.1080/10106049.2015.1130086>.
- Hong, H., Pradhan, B., Sameen, M.I., Chen, W. and Xu, C. (2017b). Spatial prediction of rotational landslide using geographically weighted regression, logistic regression, and support vector machine models in Xing Guo area (China). *Geomat. Natl. Hazar. Risk*, v.8(2), pp.1997-2022. <https://doi.org/10.1080/19475705.2017.1403974>.
- Lee, S. (2007). Application and verification of fuzzy algebraic operators to landslide susceptibility mapping. *Environmen. Geol.*, v.52, pp.615-623. <https://doi.org/10.1007/s00254-006-0491-y>.
- Lee, S.A.R.O. (2005). Application of logistic regression model and its validation for landslide susceptibility mapping using GIS and remote sensing data. *Internatl. Jour. Rem. Sens.*, v.26(7), pp.1477-1491. <https://doi.org/10.1080/01431160412331331012>.
- Lee, S. and Min, K. (2001). Statistical analysis of landslide susceptibility at Yongin, Korea. *Environmen. Geol.*, v.40, pp.1095-1113. <https://doi.org/10.1007/s002540100310>.
- Lee, S. and Pradhan, B. (2007). Landslide hazard mapping at Selangor, Malaysia using frequency ratio and logistic regression models. *Landslides*, v.4(1), pp.33-41.
- Lee, S. and Talib, J.A. (2005). Probabilistic landslide susceptibility and factor effect analysis. *Environment. Geol.*, v. 47, pp.982-990.
- Martha, T.R., Roy, P., Jain, N., Khanna, K., Mrinalni, K., Kumar, K.V. and Rao, P.V.N. (2021). Geospatial landslide inventory of India - an insight into occurrence and exposure on a national scale. *Landslides*, v.18(6), pp.2125-2141. <https://doi.org/10.1007/s10346-021-01645-1>.
- Meena, S.R., Ghorbanzadeh, O. and Blaschke, T. (2019). A comparative study of statistics-based landslide susceptibility models: A case study of the region affected by the gorkha earthquake in nepal. *ISPRS Internatl. Jour. Geo-informat.*, v.8(2), p.94. <https://doi.org/10.3390/ijgi8020094>.
- Mengistu, F., Suryabagavan, K.V., Raghuvanshi, T.K. and Lewi, E. (2019). Landslide Hazard zonation and slope instability assessment using optical and In SAR data: a case study from Gidole town and its surrounding areas, southern Ethiopia. *Rem. Sens. Land.*, v.3(1), pp.1-14. <https://doi.org/10.21523/gcj1.19030101>.
- Nohani, E., Moharrami, M., Sharafi, S., Khosravi, K., Pradhan, B., Pham, B.T., Lee, S. and M. Melesse, A. (2019). Landslide susceptibility mapping using different GIS-based bivariate models. *Water*, v. 11(7), p.1402.
- Panchal, S. and Shrivastava, A.K. (2022). Landslide hazard assessment using analytic hierarchy process (AHP): A case study of National Highway 5 in India. *Ain Shams Engineer. Jour.*, v.13(3), p.101626. <https://doi.org/10.1016/j.asej.2021.10.021>.
- Pradhan, B. and Lee, S. (2010). Delineation of landslide hazard areas on Penang Island, Malaysia, by using frequency ratio, logistic regression, and artificial neural network models. *Environment. Earth Sci.*, v.60, pp.1037-1054. <https://doi.org/10.1007/s12665-009-0245-8>.
- Saha, A.K., Gupta, R.P., Sarkar, I., Arora, M.K. and Csaplovics, E. (2005). An approach for GIS-based statistical landslide susceptibility zonation—with a case study in the Himalayas. *Landslides*, v.2, pp.61-69. <https://doi.org/10.1007/s10346-004-0039-8>.
- Uchenna, U.P., Lancia, M., Viaroli, S., Ugbaja, A.N., Galluzzi, M. and Zheng, C. (2023). Groundwater sustainability in African Metropolises: Case study from Calabar, Nigeria. *Jour. Hydrol.: Region. Stud.*, v.45, p.101314. <https://doi.org/10.1016/j.ejrh.2023.101314>.
- Yalcin, A. (2011). A geotechnical study on the landslides in the Trabzon Province, NE, Turkey. *Appl. Clay Sci.*, v.52(1-2), pp.11-19. <https://doi.org/10.1016/j.clay.2011.01.015>.
- Yang, Z. and Qiao, J. (2010). August. Regional landslide zonation based on entropy method in Three Gorges area, China. In: 2010 Seventh International Conference on Fuzzy Systems and Knowledge Discovery, v.3, pp. 1336-1339. <https://doi.org/10.1109/FSKD.2010.5569097>.
- Yu, X. and Gao, H. (2020). A landslide susceptibility map based on spatial scale segmentation: A case study at Zigui-Badong in the Three Gorges Reservoir Area, China. *PLoS One*, v.15(3), p.e0229818. <https://doi.org/10.1371/journal.pone.0229818>.